Journal of Dispersion Science and Technology

ISSN: (Print) (Online) Journal homepage: https://www.tandfonline.com/loi/ldis20

NMR investigation of counterion binding to undecyl LL-leucinevalanate micelles

Jessica Fletcher, Grant Mahant, Tyler Witzleb, Riley Busche, Mauro Garcia, Yayin Fang, Eugene J. Billiot, Fereshteh H. Billiot & Kevin F. Morris

To cite this article: Jessica Fletcher, Grant Mahant, Tyler Witzleb, Riley Busche, Mauro Garcia, Yayin Fang, Eugene J. Billiot, Fereshteh H. Billiot & Kevin F. Morris (2022): NMR investigation of counterion binding to undecyl LL-leucinevalanate micelles, Journal of Dispersion Science and Technology, DOI: 10.1080/01932691.2022.2145303

To link to this article: https://doi.org/10.1080/01932691.2022.2145303

JOURNAL OF DISPERSION SCIENCE AND TECHNOLOGY
https://doi.org/10.1080/01932691.2022.2145303

NMR investigation of counterion binding to undecyl LL-leucinevalanate micelles

Jessica Fletcher[a], Grant Mahant[a], Tyler Witzleb[a], Riley Busche[a], Mauro Garcia[b], Yayin Fang[c], Eugene J. Billiot[b], Fereshteh H. Billiot[b], and Kevin F. Morris[a]

[a]Department of Chemistry, Carthage College, Kenosha, WI, USA; [b]Department of Physical and Environmental Sciences, Texas A&M University-Corpus Christi, Corpus Christi, TX, USA; [c]Department of Biochemistry and Molecular Biology, Howard University College of Medicine, Howard University, Washington, DC, USA

ABSTRACT

NMR spectroscopy was used to investigate the binding of cationic counterions to anionic micelles formed by undecyl LL-leucinevalaninate (und-LV). Amino acid-based surfactants like und-LV are green alternatives to commercial surfactants. Monomeric and polymeric forms of und-LV micelles have also been used as chiral selectors in capillary electrophoresis (CE) separations. The counterions investigated were Na^+, the tetraethylammonium ion, L-Lysine, 1,4-diaminobutane, 1,6-diaminohexane, and cis and trans isomers of 1,2-diaminocyclohexane and 1,4-diaminocyclohexane. NMR measurements of counterion and micelle diffusion coefficients were used to calculate micelle radii and the mole fraction of counterion molecules bound to the micelles. Two-dimensional NMR experiments were used to investigate the structures of the counterion: micelle complexes. The mole fraction of bound counterions did not change with pH in solutions containing Na^+ or tetraethylammonium counterions. With all other counterions, however, the mole fraction of micelle-bound counterions was higher below pH 10 when counterions had a +1 or +2 charge, and lower above pH 10–10.5 when the counterions were neutral or zwitterionic. Changes in micelle radii with pH and two-dimensional NMR experiments suggested that L-Lysine, 1,4-diaminobutane, and 1,6-diaminohexane bound parallel to the micelle surface with their amine functional groups interacting with different surfactant monomers. In contrast, the diaminocyclohexane isomers were found to bind perpendicular to the micelle surface. The mole fractions of micelle-bound cis-1,4-diaminocyclohexane and trans-1,4-diaminocyclohexane were very similar to one another. However, with 1,2-cyclohexanediamine, at low pH the mole fraction of micelle-bound counterions was larger for the cis isomer than for the trans isomer.

GRAPHICAL ABSTRACT

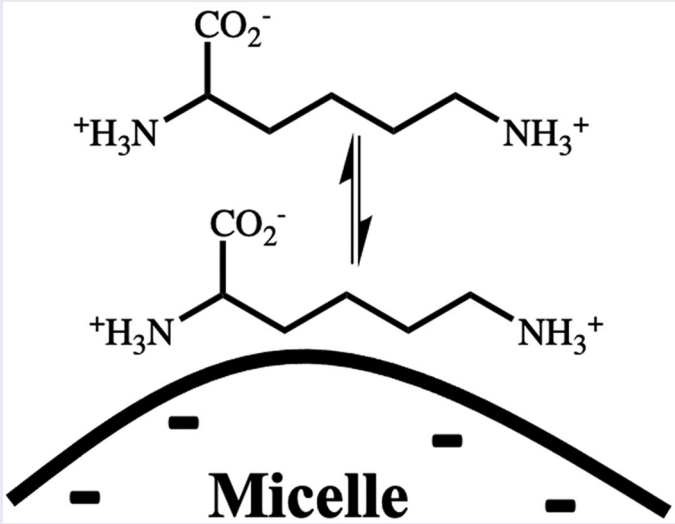

ARTICLE HISTORY
Received 11 August 2022
Accepted 3 November 2022

KEYWORDS
NMR; diffusion; amino acid-based surfactant; counterion

Introduction

Surfactants are used throughout the cosmetics, personal care, agricultural, and petroleum industries because their amphiphilic properties facilitate the mixing of oil and water phases. As a result, surfactants stabilize many commercial formulations and dispersions.[1] Many of these applications currently use synthetic surfactants partially derived from nonrenewable fossil fuels. Industries, however, are seeking

CONTACT Kevin F. Morris kmorris@carthage.edu Department of Chemistry, Carthage College, 2001 Alford Park Drive, Kenosha, WI 53140, USA
Supplemental data for this article can be accessed online at https://doi.org/10.1080/01932691.2022.2145303

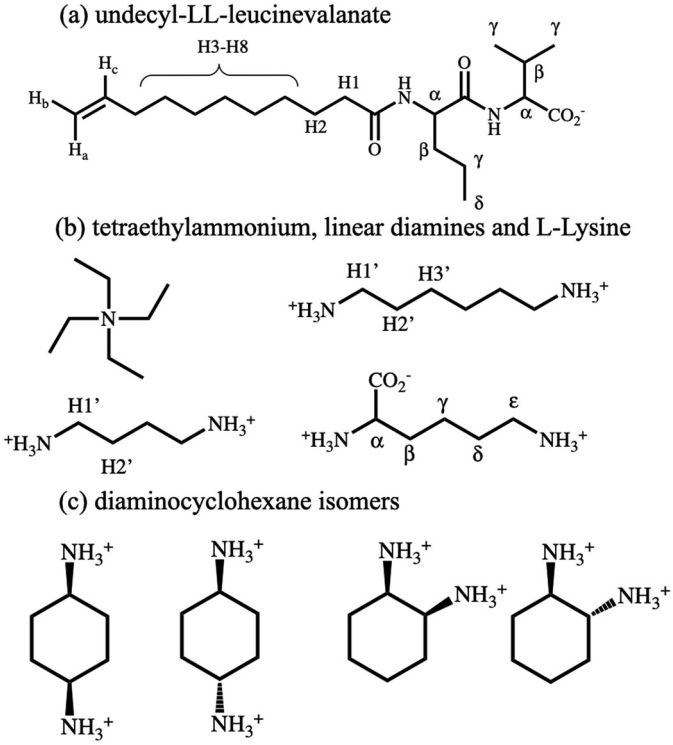

Figure 1. Chemical structures of (a) undecyl-LL-leucinevalanate; (b) linear diamines and L-Lysine, and (c) cyclohexanediamine isomers.

greener alternatives where surfactant molecules are produced from natural oils, biomass, or by microorganisms. Examples of green surfactants include rhamnolipids, sophorolipids, alkly polyglucosides, and amino acid-based surfactants.[2] In the latter, an amino acid or small peptide is connected through an amide, ester, or other linkage to a hydrocarbon chain. Amino acid-based surfactants have been shown to be biodegradable and environmentally benign and can often be produced from abundant, sustainable materials.[3–8] Some amino acid-based surfactants also have antimicrobial properties.[9]

The amino acid-based surfactant investigated here is undecyl LL-leucinevalanate (und-LV). The surfactant's molecular structure is shown in Figure 1a. Protons labels are used to assign the NMR spectra. Und-LV contains an C11 hydrocarbon chain connected by an amide bond to a dipeptide leucinevalinate head group. Since the Cα of each amino acid in the und-LV headgroup is a chiral center, micelles of und-LV have been used as chiral selectors in capillary electrophoresis (CE) separations.[10,11] In these experiments, micelles formed from chiral surfactants and a racemic analyte mixture are pulled down a capillary tube by an electric field. When the enantiomers in the mixture interact differently with the micelle's chiral headgroup atoms, the enantiomers travel through the capillary with different velocities and are separated from one another.[12] Und-LV micelles containing both monomeric and polymeric surfactants have been used in chiral CE separations.[10,11] Molecular modeling, fluorescence anisotropy, and NMR spectroscopy have also been used to characterize the interactions of chiral compounds with und-LV micelles. In these studies, both experimental and modeling work showed that the surfactant's dipeptide headgroup adopted a folded conformation by turning its Leucine side chain toward the micelle core. This conformation resulted in the formation of a chiral pocket into which chiral ligands inserted. Within these chiral pockets, the formation of stereoselective hydrogen bonds between the ligand enantiomers and surfactant headgroup atoms was an important factor governing chiral discrimination.[13–17]

At basic pH, the carboxylic acid functional group on the und-LV headgroup is deprotonated, giving each surfactant monomer and the surface of und-LV micelles a negative charge. Positive alkali metal cations and organic cations like amines and amino acids bind to this anionic micelle surface. Previous studies have shown that the binding of counterions to micelles affects their physical properties. For example, Jansson and Stilbs showed that the CMC of decylammonium surfactants decreased as the size and polarity of the acetate counterions present in solution increased.[18] Koyama obtained similar results when investigating the critical micelle concentration (CMC) of fatty acids in the presence of L-Arginine and alkali metal cations. Again, the surfactant CMC was lowered in the presence of the larger L-Arginine counterions.[19] In addition, the binding of triflate counterions caused normally spherical dodecyltrimethylammonium micelles to adopt a disk-like shape and eventually precipitate from solution.[20] The effect of counterion hydrophobicity on the aggregation of polyelectrolyte micelles and the role played by counterion-surfactant ion pairs in micelle formation have been investigated as well.[21–23] Finally, NMR experiments have provided estimates of the diffusion coefficients of metal cations along anionic micelle surfaces.[24,25]

Micelle counterions have also been shown to affect the chiral resolution of binaphthyl enantiomers in separations using the amino acid-based surfactant undecyl L-Leucinate as the pseudostationary phase. These studies showed that chiral resolution of the enantiomers was higher when either L-Arginine or L-Lysine counterions were bound to the micelle surface. Chiral resolution was lower when Na^+ counterions were present. In addition, chiral resolution also decreased at high pH when L-Arginine and L-Lysine were no longer bound to the micelles. These studies show that when amino acid-based surfactants are used in chiral separations, the micelle counterion present in solution must be carefully considered.[26,27]

In this study, NMR spectroscopy was used to characterize the interactions between eight cationic amine counterions and und-LV micelles as a function of solution pH. An experiment was also performed with und-LV micelles and Na^+ counterions for reference. The structures of the counterions investigated are shown in Figure 1b and 1c. Proton labels are shown for the linear diamines and L-Lysine. These counterions include one quaternary amine, two linear diamines, an amino acid, and the cis and trans isomers of 1,2- and 1,4-diaminocyclohexane. Studies were carried out as a function of pH because und-LV contains carboxylic acid and amide functional groups, so the charge and packing of the headgroups in micelles formed by this surfactant would be expected to change with pH. The charges of the counterions should be

pH dependent as well.[28,29] The overall goal of this study was to understand how pH conditions affected the association of the counterions shown in Figure 1b and 1c with the anionic und-LV micelle surface. A further goal was to characterize the structures of the micelle-counterion complexes formed by the molecules in Figure 1 under pH conditions where the counterions were bound to the und-LV micelles.

Characterizing how the physical properties of amino acid-based micelles change with counterion and pH is necessary for their optimal use in commercial products. In addition, recent studies have shown that when und-LV was used as a chiral selector in capillary CE separations, greater resolution of enantiomers was achieved by careful selection of the micelle counterion and pH conditions.[26,27] This study was undertaken to better characterize chiral surfactant-counterion interactions and thus give separation scientist the additional tools needed to choose the optimal solution conditions for chiral CE separations.

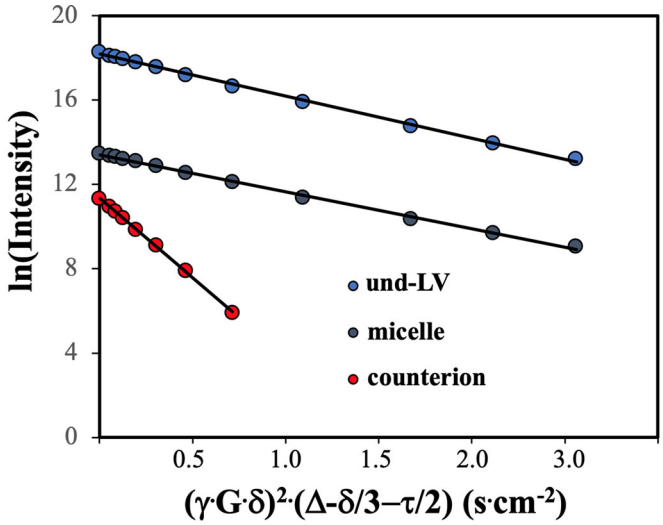

Figure 2. ln(Intensity) versus $(\gamma G\delta)^2 \cdot (\Delta - \delta/3 - \tau/2)$ plot for a solution containing und-LV micelles, TMS, and 1,6-diaminohexane. The slope of each plot is –D.

Materials and methods

Deuterium oxide (99.9 atom %D), 1,6-diaminohexane (99%), 1-4-diaminobutane (99%), L-Lysine (98%), trans-1,2-diaminocyclohexane, tetramethyl silane (>99.9%), NaOH (97%), and $DCl_{(aq)}$ (35 wt% solution in D_2O, > 99.9% atom %D) were purchased from Sigma-Aldrich. cis-1,2-diaminocyclohexane was purchased from Acros Organics, Inc. and CHEM-IMPEX International, Inc. provided cis- and trans-1,4-diaminocyclohexane. The surfactant undecyl LL-leucinevalaninate (und-LV) was synthesized and purified by methods previously described.[28] A proton NMR spectrum of a mixture of 50.0 mM und-LV and $NaHCO_{3(aq)}$ at pH 9.0 is shown in Figure 1 of the Supplemental Information.

Solutions for NMR analysis were prepared gravimetrically and contained 50.0 mM of und-LV, 50 mM $NaHCO_{3(aq)}$ and 25 mM of one of the counterions in Figure 1. The solvent was 90% H_2O/10% D_2O. Solution pH was adjusted by adding either small amounts of $NaOH_{(s)}$ or 37 wt% $DCl_{(aq)}$ to the solutions. A Denver Instruments pH meter that was three-point calibrated before each experiment was used for all pH measurements. Samples at each desired pH were transferred into NMR tubes and spiked with a small amount of tetramethylsilane (≥99.9%) (TMS). The TMS molecules were solubilized inside the micelle's hydrophobic core and were used to measure the diffusion coefficients of the micelles.[30–35] Solutions were allowed to equilibrate at 25.0 °C before NMR measurements were made.

All NMR experiments were done on a Bruker 400 MHz spectrometer. Diffusion coefficient measurements were made by collecting spectra with increasing gradient strength, G, using the bipolar pulse pair longitudinal encode–decode pulse sequence.[36] Eighteen spectra were collected in each experiment with G ranging from 2.0 to 40.0 G·cm^{-1}. The total duration of the bipolar gradient pulses was 4.0 ms, the delay τ between the bipolar pulses was 0.2 ms, and the diffusion time, Δ, was 250.0 ms. Each spectrum contained 64k points with a SW of 8012 Hz. After data acquisition, free induction decays were apodized with 0.3 Hz line broadening, Fourier transformed, phased, and baseline corrected. The intensities of the surfactant hydrocarbon chain, TMS, and counterion resonances were then recorded for each gradient amplitude. Graphs were prepared of the natural log of peak intensity versus the quantity $(\gamma \cdot G \cdot \delta)^2 \cdot (\Delta - \delta/3 - \tau/2)$, where γ is the magnetogyric ratio.[36] The slope of each of these plots was –D, where D is the respective component's diffusion coefficient. Linear regression analyses were used to calculate each D value. A representative plot ln of peak intensity versus $(\gamma \cdot G \cdot \delta)^2 \cdot (\Delta - \delta/3 - \tau/2)$ for a solution containing 50.0 mM und-LV, 25.0 mM 1,6-diaminohexane, and TMS is shown in Figure 2. Three replicate measurements were made for each solution.

In the Rotating Frame Overhauser Enhanced Spectroscopy (ROESY) experiments, a phase sensitive pulse sequence with WATERGATE H_2O suppression and a spin lock time of 200 ms was used.[37,38] Each FID in the f2 dimension was collected with 256 transients, 2k data points, and a spectral width of 4000 Hz. A total of 256 increments were used in the f1 dimension. Linear prediction was used to extend the data set in the f1 dimension by 200 points and zero filling was carried out to generate a 2048 × 1024 point data set. The data set was then apodized with a $\pi/2$-shifted sine-bell-squared function, before being Fourier transformed and phased in both dimensions.

Results and discussion

Micelle radii and counterion binding

NMR diffusion experiments were performed using solutions containing 50 mM und-LV and 25 mM of each counterion. Diffusion coefficients for the micelle, counterion, and surfactant were then independently measured by monitoring the decay of the intensity of the respective component's NMR resonance with increasing gradient strength.[30,36] Surfactant molecules undergo dynamic exchange between free solution and the micelle-bound state. Therefore, as shown in Equation (1), the diffusion coefficient measured by monitoring the decay of the surfactant resonances ($D_{obs,LV}$) is the

weighted average of the free solution ($D_{free,LV}$) and micelle-bound ($D_{micelle}$) values.[30,31,33]

$$D_{obs,LV} = f_{b,LV} \cdot D_{micelle} + (1 - f_{b,LV}) \cdot D_{free,LV} \quad [1]$$

In Equation (1), $f_{b,LV}$ is the mole fraction of und-LV monomers bound to the surfactant. The und-LV free solution diffusion coefficient was found to be $(5.58 \pm 0.02) \times 10^{-10}$ m^2s^{-1} in a diffusion experiment with the und-LV concentration below the surfactant's CMC. $D_{micelle}$ was measured by spiking each solution with a small amount of TMS. Since the TMS molecules are solubilized inside the nonpolar micelle core, the decay of the TMS resonance amplitude with increasing gradient strength is a measure of the diffusion coefficient of the micelle.[30–35] Finally, $f_{b,LV}$ was then calculated with Equation (1). The D values in Equation (1) are defined above.

$D_{micelle}$ values and the Stokes–Einstein relation (Equation (2)) were used to calculate the micelle hydrodynamic radius, R_h, at each pH investigated.

$$D_{micelle} = \frac{k_B \cdot T}{6 \cdot \pi \cdot \eta \cdot R_h} \quad [2]$$

This calculation yields the radius of the sphere with the same diffusion coefficient as the micelle.[30,39] In Equation (2), $D_{micelle}$ is measured as described above, k_B is Boltzmann's constant, T is absolute temperature, and η is the viscosity. Viscosity values for solutions containing amino acid-based surfactants have been reported previously.[28] In these experiments, an Oswald viscometer was used to measure the viscosities of 50.0 mM solutions of undecyl L-Leucinate in 90% H_2O/10% D_2O over the pH range 6.69–11.62. The viscosity was found to be constant over this pH range. The average of these viscosity measurements was 1.06 ± 0.02 cp. This η value was used for all radius calculations reported here. A previous study of the amino acid-based surfactant undecyl L-Phenylalaninate also used these viscosities to calculate R_h.[29]

Equation (3) can be written for the observed diffusion coefficient of each counterion in the presence of the und-LV micelles, $D_{obs,counterion}$.[28–31,35]

$$D_{obs,counterion} = f_{b,counterion} \cdot D_{micelle} + (1 - f_{b,counterion}) \cdot D_{free,counterion} \quad [3]$$

Equation (3) holds because, like the und-LV surfactant monomers, counterions bound to the micelle surface also undergo fast exchange on the NMR timescale between free solution and micelle-bound states. $D_{obs,counterion}$ values were measured by monitoring the decay of counterion resonances with increasing gradient strength. $D_{micelle}$ was measured as described above, and $D_{free,counterion}$ was measured by carrying out an experiment with a solution containing only the counterion and no und-LV micelles. $D_{free,counterion}$ values are given in Table 1 of the Supplemental Information. In Equation (3), $f_{b,counterion}$ is the mole fraction of counterion molecules bound to the micelles. These values along with hydrodynamic radii are reported as a function of pH for each counterion investigated.

TEA, linear diamines, and L-lysine

Table 1 shows $D_{obs,LV}$, $D_{micelle}$, $f_{b,LV}$, and R_h values derived from Equations (1) and (2), respectively, as a function of pH for und-LV micelles with Na^+ counterions. The solutions investigated contained 50.0 mM und-LV and 50.0 mM $NaHCO_3$. The $f_{b,LV}$ values were observed to fall between 0.92 and 0.95 in the pH range investigated and the hydrodynamic radii fell between 11.5 and 13.0 Å. These results suggest that in solutions with Na^+ counterions, pH has little effect on the radii of the micelles and that the fraction of surfactant monomers associated with micelles remains near one from pH 7.5 to 11.5. The latter result is also observed for all other counterions investigated. Figures 3 and 4 show plots of $f_{b,LV}$, $f_{b,counterion}$, and R_h versus pH for tetraethylammonium counterions (Figure 3A), the two linear diamines (Figure 3B and 3C), L-Lysine (Figure 3D) and the cyclohexanediamine isomers (Figure 4). Corresponding numerical values and diffusion coefficients are shown in Tables 1–4. The TEA, linear diamine, and L-Lysine counterions will be discussed first, followed by an examination of the behavior of the 1,4-cyclohexanediamine and 1,2-cyclohexanediamine isomers.

Figure 3A shows plots of $f_{b,LV}$, $f_{b,counterion}$, and R_h versus pH for und-LV-TEA mixtures from pH 7.5 to 11.5. Corresponding numerical values and diffusion coefficients are shown in Table 1. Since TEA is a quaternary amine, it is cationic at all pH values, so the fraction of TEA counterions bound to the micelles would be expected to remain relatively constant with pH. This trend is observed in Table 1 and Figure 3A, with $f_{b,counterion}$ remaining between 0.32 and 0.34 in the pH range investigated. The hydrodynamic radii of the micelles in solutions containing TEA counterions are also marginally larger than corresponding radii when only Na^+ was bound to the micelle surface and do not change substantially with pH.

The fraction of micelle-bound counterions, however, does change as a function of pH in solutions containing 1,6-diaminohexane ($pK_{a1} = 11.86$, $pK_{a2} = 10.76$), 1,4-diaminobutane ($pK_{a1} = 10.80$, $pK_{a2} = 9.63$), and L-Lysine ($pK_{a1} = 2.16$, $pK_{a2} = 9.06$, $pK_{a3} = 10.54$) counterions.[40] The pK_a values in parentheses indicate that the amine functional groups for 1,6-diaminohexane and 1,4-diaminobutane are in their protonated or ammonium state below pH ~10. The counterions in this pH range are thus cationic. Deprotonation at higher pH reduces the counterion charge. In L-Lysine, both of the amine functional groups are in protonated or ammonium states below pH ~ 9. In this pH range L-Lysine has an overall +1 charge because of the anionic carboxylate functional group. At higher pH, the amine functional groups deprotonate and the L-Lysine counterion becomes zwitterionic. Figures 3B and Table 2 show that the 1,6-diaminohexane $f_{b,counterion}$ values are in the range 0.51–0.56 from pH 7.5 to 10, indicating that at these pH values the cationic amine is relatively strongly bound to the anionic micelle surface. The fraction of bound counterions, however, begins to decrease above pH 10, reaching a value of only 0.15 at pH 11.5. Therefore, as the diamine deprotonates it becomes less attracted to the micelle

Table 1. $D_{obs,LV}$, $D_{micelle}$, $f_{b,LV}$, and hydrodynamic radii from pH 7.5 to 11.5 for solutions containing 50.0 mmol und-LV and 50.0 mM $NaHCO_3$

Na^+ counterions				
pH	$D_{obs,LV} \times 10^{-10}$ ($m^2 \cdot s^{-1}$)	$D_{micelle} \times 10^{-10}$ ($m^2 \cdot s^{-1}$)	$f_{b,LV}$	R_h (Å)
7.5	1.79 ± 0.01	1.52 ± 0.01	0.92 ± 0.01	12.6 ± 0.3
8.0	1.81 ± 0.01	1.58 ± 0.01	0.94 ± 0.01	12.2 ± 0.2
8.5	1.85 ± 0.01	1.64 ± 0.01	0.94 ± 0.01	11.7 ± 0.2
9.0	1.86 ± 0.02	1.68 ± 0.02	0.95 ± 0.01	11.4 ± 0.3
9.5	1.82 ± 0.01	1.67 ± 0.02	0.95 ± 0.01	11.5 ± 0.3
10.0	1.76 ± 0.01	1.58 ± 0.01	0.95 ± 0.01	12.2 ± 0.2
10.5	1.74 ± 0.01	1.53 ± 0.01	0.94 ± 0.01	12.5 ± 0.3
11.0	1.70 ± 0.01	1.48 ± 0.02	0.94 ± 0.01	13.0 ± 0.3
11.5	1.70 ± 0.01	1.47 ± 0.01	0.94 ± 0.01	13.0 ± 0.3
Tetraethylammonium counterions				
pH	$D_{obs,LV} \times 10^{-10}$ ($m^{2*}s^{-1}$)	$D_{micelle} \times 10^{-10}$ ($m^{2*}s^{-1}$)	$D_{obs,counterion} \times 10^{-10}$ ($m^{2*}s^{-1}$)	$f_{b,counterion}$	R_h(Å)
7.5	1.70 ± 0.02	1.41 ± 0.02	7.29 ± 0.09	0.34 ± 0.02	14.9 ± 0.4
8.0	1.60 ± 0.01	1.38 ± 0.05	7.49 ± 0.07	0.32 ± 0.01	15.1 ± 0.6
8.5	1.61 ± 0.02	1.31 ± 0.01	7.43 ± 0.07	0.32 ± 0.02	15.8 ± 0.6
9.0	1.70 ± 0.02	1.56 ± 0.03	7.43 ± 0.03	0.33 ± 0.03	13.2 ± 0.3
9.5	1.66 ± 0.03	1.39 ± 0.04	7.46 ± 0.02	0.32 ± 0.05	14.9 ± 0.4
10.0	1.65 ± 0.03	1.37 ± 0.05	7.37 ± 0.04	0.33 ± 0.01	15.1 ± 0.6
10.5	1.56 ± 0.01	1.31 ± 0.05	7.47 ± 0.09	0.32 ± 0.02	15.8 ± 0.6
11.0	1.51 ± 0.01	1.61 ± 0.02	7.49 ± 0.04	0.33 ± 0.01	13.0 ± 0.2
11.5	1.43 ± 0.01	1.55 ± 0.05	7.52 ± 0.08	0.33 ± 0.02	13.3 ± 0.4

$D_{obs,LV}$, $D_{micelle}$, $D_{obs,counterion}$, $f_{b,counterion}$, and hydrodynamic radii in the same pH range for solutions containing 50.0 mmol und-LV and 50.0 mM tetraethylammonium counterions. All uncertainties were calculated from three replicate measurements.

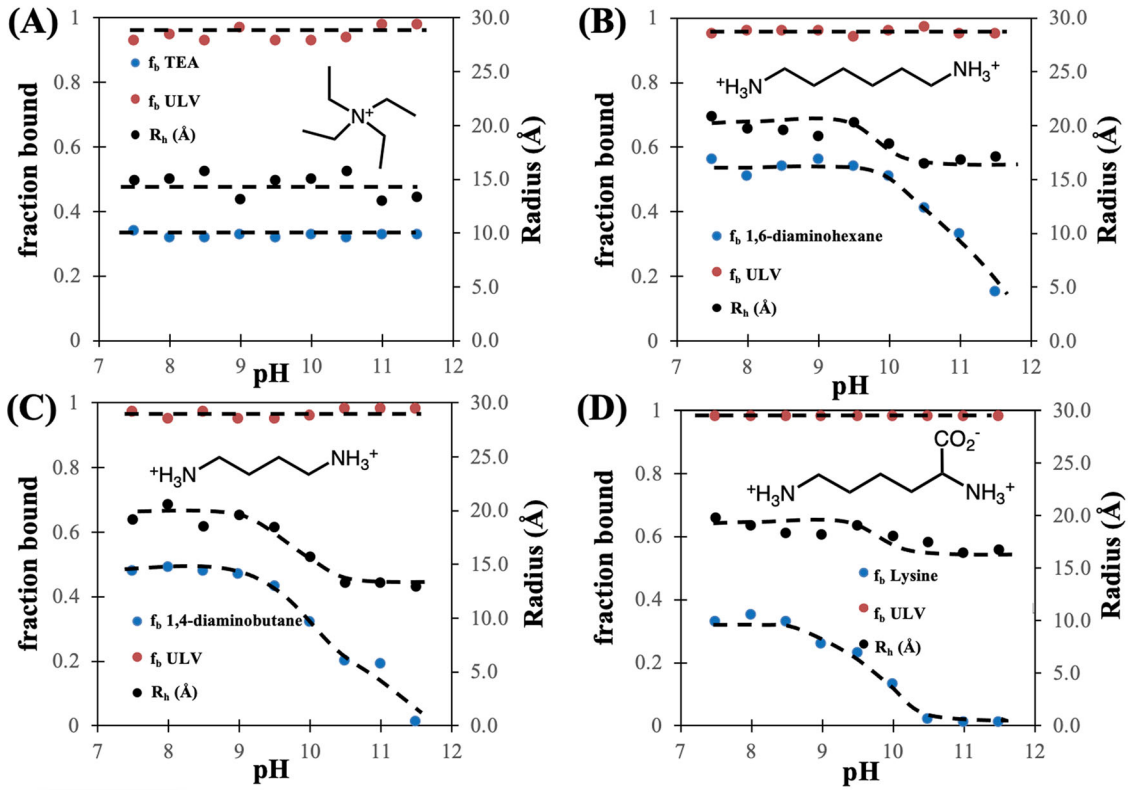

Figure 3. Plots of $f_{b,LV}$, $f_{b,counterion}$, and R_h for und-LV solutions containing (A) tetraethylammonium, (B) 1,6-diaminohexane, (C) 1,4-diaminohexane, and (D) L-Lysine counterions.

surface and the fraction of bound counterion molecules decrease. Similar results are obtained with 1,4-diaminobutane counterions (Table 2 and Figure 3C) where $f_{b,counterion}$ values are in the range 0.49–0.43 below pH 10. At higher pH $f_{b,counterion}$ decreases to zero at pH 11.5. At this pH, the diamine counterions have dissociated completely from the micelle surface and have been replaced with Na^+ cations. Finally, $f_{b,LV}$ remains above 0.90 throughout the pH range investigated in experiments with both 1,6-diaminohexane and 1,4-diaminobutane, indicating that pH does not affect the fraction of und-LV monomer associated with the micelles. D values used to calculate $f_{b,counterion}$ and R_h for both linear diamine counterions are also given in Table 2.

Plots of $f_{b,counterion}$, $f_{b,LV}$, and R_h versus pH for solutions containing und-LV micelles and L-Lysine are shown in Figure 3D. Numerical values for $f_{b,counterion}$ and R_h and

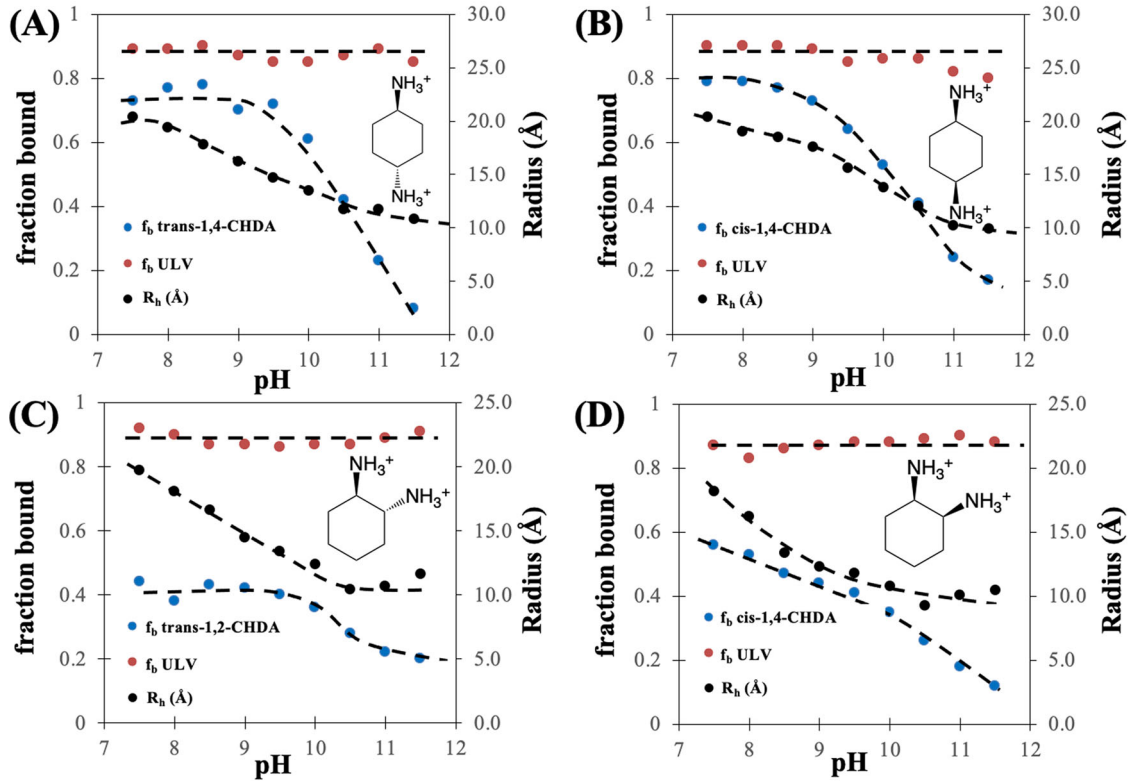

Figure 4. Plots of $f_{b,LV}$, $f_{b,counterion}$, and Rh for und-LV solutions containing (A) trans-1,4-diaminocyclohexane, (B) cis-1,4-diaminocyclohexane, (C) trans-1,2-diaminocyclohexane, and (D) cis-1,2-diaminocyclohexane.

Table 2. $D_{obs,LV}$, $D_{micelle}$, $D_{obs,counterion}$, $f_{b,counterion}$, and hydrodynamic radii in the pH range 7.5–11.5 for solutions containing 50.0 mmol und-LV and 25.0 mM of either 1,6-diaminohexane, 1,4-diaminobutane, or L-Lysine

1,6-diaminohexane					
pH	$D_{obs,LV} \times 10^{-10}$ (m^2*s^{-1})	$D_{micelle} \times 10^{-10}$ (m^2*s^{-1})	$D_{obs,counterion} \times 10^{-10}$ (m^2*s^{-1})	$f_{b,counterion}$	R_h (Å)
7.5	1.19 ± 0.01	1.00 ± 0.03	4.49 ± 0.01	0.56 ± 0.01	20.8 ± 0.04
8.0	1.22 ± 0.01	1.05 ± 0.02	4.94 ± 0.01	0.51 ± 0.01	19.7 ± 0.02
8.5	1.22 ± 0.01	1.05 ± 0.01	4.73 ± 0.02	0.54 ± 0.02	19.6 ± 0.01
9.0	1.25 ± 0.01	1.09 ± 0.01	4.58 ± 0.01	0.56 ± 0.01	19.0 ± 0.01
9.5	1.25 ± 0.02	1.02 ± 0.06	4.69 ± 0.02	0.54 ± 0.02	20.3 ± 0.05
10.0	1.30 ± 0.02	1.13 ± 0.03	4.94 ± 0.03	0.51 ± 0.03	18.3 ± 0.04
10.5	1.38 ± 0.01	1.26 ± 0.01	5.56 ± 0.01	0.41 ± 0.01	16.5 ± 0.02
11.0	1.33 ± 0.02	1.23 ± 0.12	5.56 ± 0.02	0.33 ± 0.02	16.8 ± 0.16
11.5	1.40 ± 0.01	1.21 ± 0.09	7.77 ± 0.01	0.15 ± 0.01	17.1 ± 0.08
1,4-diaminobutane					
7.5	1.21 ± 0.01	1.08 ± 0.03	5.75 ± 0.04	0.48 ± 0.01	19.1 ± 0.01
8.0	1.20 ± 0.01	1.00 ± 0.03	5.64 ± 0.05	0.49 ± 0.01	20.6 ± 0.01
8.5	1.25 ± 0.01	1.12 ± 0.04	5.78 ± 0.03	0.48 ± 0.01	18.5 ± 0.01
9.0	1.25 ± 0.01	1.05 ± 0.03	5.82 ± 0.02	0.47 ± 0.01	19.6 ± 0.01
9.5	1.31 ± 0.01	1.12 ± 0.03	6.19 ± 0.01	0.43 ± 0.01	18.4 ± 0.01
10.0	1.46 ± 0.01	1.33 ± 0.03	7.28 ± 0.10	0.32 ± 0.01	15.6 ± 0.01
10.5	1.62 ± 0.01	1.56 ± 0.02	8.34 ± 0.10	0.20 ± 0.01	13.3 ± 0.01
11.0	1.51 ± 0.01	1.56 ± 0.02	8.43 ± 0.06	0.19 ± 0.01	13.3 ± 0.01
11.5	1.63 ± 0.01	1.61 ± 0.03	9.30 ± 0.01	0.0	12.9 ± 0.01
L-Lysine					
7.5	1.20 ± 0.01	1.05 ± 0.01	4.81 ± 0.01	0.33 ± 0.01	19.7 ± 0.1
8.0	1.23 ± 0.03	1.09 ± 0.01	5.01 ± 0.02	0.35 ± 0.01	19.0 ± 0.2
8.5	1.22 ± 0.01	1.13 ± 0.01	5.49 ± 0.01	0.33 ± 0.02	18.3 ± 0.1
9.0	1.21 ± 0.01	1.14 ± 0.01	5.71 ± 0.01	0.26 ± 0.01	18.2 ± 0.1
9.5	1.27 ± 0.03	1.09 ± 0.01	6.32 ± 0.05	0.23 ± 0.01	19.0 ± 0.2
10.0	1.29 ± 0.01	1.15 ± 0.01	6.94 ± 0.01	0.13 ± 0.01	18.0 ± 0.2
10.5	1.27 ± 0.01	1.19 ± 0.01	7.06 ± 0.02	0.02 ± 0.01	17.4 ± 0.1
11.0	1.26 ± 0.01	1.26 ± 0.01	7.08 ± 0.03	0.0	16.4 ± 0.1
11.5	1.25 ± 0.03	1.24 ± 0.01	7.08 ± 0.01	0.0	16.7 ± 0.2

All uncertainties were calculated from three replicate measurements.

Table 3. $D_{obs,LV}$, $D_{micelle}$, $D_{obs,counterion}$, $f_{b,counterion}$, and hydrodynamic radii in the pH range 7.5–11.5 for solutions containing 50.0 mmol und-LV and 25.0 mM of either trans-1,4-diaminocyclohexane or cis-1,4-diaminocyclohexane

pH	$D_{obs,LV} \times 10^{-10}$ (m^2*s^{-1})	$D_{micelle} \times 10^{-10}$ (m^2*s^{-1})	$D_{obs,counterion} \times 10^{-10}$ (m^2*s^{-1})	$f_{b,counterion}$	R_h (Å)
Trans-1,4-cyclohexanediamine					
7.5	2.24 ± 0.02	1.03 ± 0.01	3.35 ± 0.07	0.73 ± 0.01	20.4 ± 0.1
8.0	2.00 ± 0.01	1.06 ± 0.01	2.95 ± 0.01	0.77 ± 0.01	19.4 ± 0.1
8.5	2.01 ± 0.01	1.16 ± 0.01	3.04 ± 0.04	0.78 ± 0.01	17.8 ± 0.1
9.0	2.32 ± 0.02	1.27 ± 0.01	3.71 ± 0.05	0.70 ± 0.02	16.2 ± 0.1
9.5	2.59 ± 0.01	1.40 ± 0.01	3.65 ± 0.02	0.72 ± 0.01	14.7 ± 0.1
10.0	2.76 ± 0.02	1.53 ± 0.01	4.65 ± 0.02	0.61 ± 0.01	13.5 ± 0.1
10.5	2.77 ± 0.06	1.76 ± 0.02	6.22 ± 0.07	0.42 ± 0.01	11.7 ± 0.2
11.0	2.68 ± 0.06	1.79 ± 0.03	7.72 ± 0.02	0.23 ± 0.01	11.7 ± 0.2
11.5	3.11 ± 0.04	1.90 ± 0.02	8.90 ± 0.04	0.08 ± 0.03	10.8 ± 0.2
Cis-1,4-cyclohexanediamine					
7.5	1.86 ± 0.02	1.01 ± 0.03	2.79 ± 0.03	0.79 ± 0.03	20.4 ± 0.3
8.0	1.95 ± 0.01	1.09 ± 0.01	2.89 ± 0.01	0.79 ± 0.01	19.0 ± 0.2
8.5	1.98 ± 0.01	1.11 ± 0.01	3.03 ± 0.02	0.77 ± 0.01	18.5 ± 0.2
9.0	2.08 ± 0.01	1.17 ± 0.01	3.42 ± 0.02	0.73 ± 0.02	17.6 ± 0.2
9.5	2.28 ± 0.03	1.32 ± 0.03	4.08 ± 0.02	0.64 ± 0.02	15.6 ± 0.6
10.0	2.64 ± 0.02	1.49 ± 0.02	5.26 ± 0.03	0.53 ± 0.02	13.8 ± 0.2
10.5	2.85 ± 0.02	1.71 ± 0.01	6.35 ± 0.04	0.41 ± 0.02	12.0 ± 0.1
11.0	3.36 ± 0.05	2.01 ± 0.02	7.71 ± 0.06	0.24 ± 0.05	10.2 ± 0.5
11.5	3.54 ± 0.04	2.08 ± 0.05	8.68 ± 0.08	0.17 ± 0.05	9.9 ± 0.5

All uncertainties were calculated from three replicate measurements.

Table 4. $D_{obs,LV}$, $D_{micelle}$, $D_{obs,counterion}$, $f_{b,counterion}$, and hydrodynamic radii in the pH range 7.5–11.5 for solutions containing 50.0 mmol und-LV and 25.0 mM of either trans-1,2-diaminocyclohexane or cis-1,2-diaminocyclohexane

pH	$D_{obs,LV} \times 10^{-10}$ (m^2*s^{-1})	$D_{micelle} \times 10^{-10}$ (m^2*s^{-1})	$D_{obs,counterion} \times 10^{-10}$ (m^2*s^{-1})	$f_{b,counterion}$	R_h (Å)
Trans-1,2-cyclohexanediamine					
7.5	1.76 ± 0.01	1.04 ± 0.01	5.81 ± 0.05	0.44 ± 0.01	19.7 ± 0.3
8.0	2.00 ± 0.01	1.14 ± 0.01	6.31 ± 0.02	0.38 ± 0.01	18.1 ± 0.1
8.5	2.34 ± 0.01	1.24 ± 0.02	5.92 ± 0.02	0.43 ± 0.01	16.6 ± 0.1
9.0	2.51 ± 0.02	1.42 ± 0.01	6.14 ± 0.02	0.42 ± 0.01	14.5 ± 0.1
9.5	2.63 ± 0.03	1.55 ± 0.01	6.34 ± 0.02	0.40 ± 0.01	13.4 ± 0.1
10.0	2.72 ± 0.01	1.66 ± 0.02	6.75 ± 0.02	0.36 ± 0.01	12.4 ± 0.1
10.5	2.99 ± 0.06	1.98 ± 0.05	7.43 ± 0.02	0.28 ± 0.01	10.4 ± 0.5
11.0	2.78 ± 0.04	1.92 ± 0.02	7.86 ± 0.02	0.22 ± 0.02	10.7 ± 0.1
11.5	2.50 ± 0.03	1.77 ± 0.05	7.96 ± 0.02	0.20 ± 0.01	11.6 ± 0.1
Cis-1,2-cyclohexanediamine					
7.5	2.14 ± 0.02	1.01 ± 0.01	4.70 ± 0.02	0.56 ± 0.01	18.4 ± 0.2
8.0	2.64 ± 0.01	1.27 ± 0.04	5.13 ± 0.04	0.53 ± 0.01	16.2 ± 0.5
8.5	2.63 ± 0.04	1.53 ± 0.01	5.61 ± 0.04	0.49 ± 0.01	13.4 ± 0.5
9.0	2.72 ± 0.01	1.68 ± 0.02	6.07 ± 0.02	0.44 ± 0.01	12.3 ± 0.2
9.5	2.72 ± 0.02	1.75 ± 0.01	6.33 ± 0.02	0.41 ± 0.01	11.8 ± 0.1
10.0	2.85 ± 0.03	1.91 ± 0.01	6.84 ± 0.03	0.35 ± 0.01	10.8 ± 0.1
10.5	3.01 ± 0.05	2.23 ± 0.03	7.67 ± 0.05	0.26 ± 0.01	9.3 ± 0.5
11.0	2.79 ± 0.03	2.03 ± 0.03	8.17 ± 0.07	0.18 ± 0.02	10.1 ± 0.2
11.5	2.84 ± 0.07	1.97 ± 0.03	8.65 ± 0.04	0.12 ± 0.01	10.5 ± 0.1

All uncertainties were calculated from three replicate measurements.

corresponding diffusion coefficients are given in Table 2. The pK_a values above indicate that L-Lysine is cationic below pH 9. Above this pH, the side chain amine functional group deprotonates and the amino acid is zwitterionic. This behavior was found to affect the amino acid's binding to the anionic und-LV surface. Below pH 9.0, $f_{b,counterion}$ for L-Lysine was in the 0.33–0.35 range. Above this pH, $f_{b,counterion}$ decreased steadily to zero at pH 11.5.

For the two linear diamines and L-Lysine, there was also only a modest decrease in the micelle hydrodynamic radius when the counterions dissociated from the micelle surface at higher pH. For example, in 1,6-diaminohexane R_h decreased from approximately 21 Å to 17 Å from pH 7.5 to 11.5. Corresponding decreases of 20 Å–13 Å and 20 Å–17 Å were observed for 1,4-diaminobutane and L-Lysine, respectively. These small changes in R_h suggest that 1,6-diaminohexane, 1,4-diaminobutane, and L-lysine all bind parallel to the micelle surface with the amine functional groups bridging two surfactant monomers. This model is shown in Figure 5a and 5b. Previous work has shown that L-lysine binds to undecyl-L-Leucinate and undecyl-L-Phenylananate micelles in a similar manner.[28,29] When the counterion then dissociates from the micelle surface at higher pH, the micelle radius changed by a small amount.

Furthermore, when the diamine or L-Lysine counterions were bound to the micelles at low pH, micelle hydrodynamic radii fell in the 18–20 Å range. This radius is comparable to the length of the und-LV surfactant monomer. The radii measurements, therefore, suggest that the linear diamine and L-Lysine counterions bind to a single und-LV

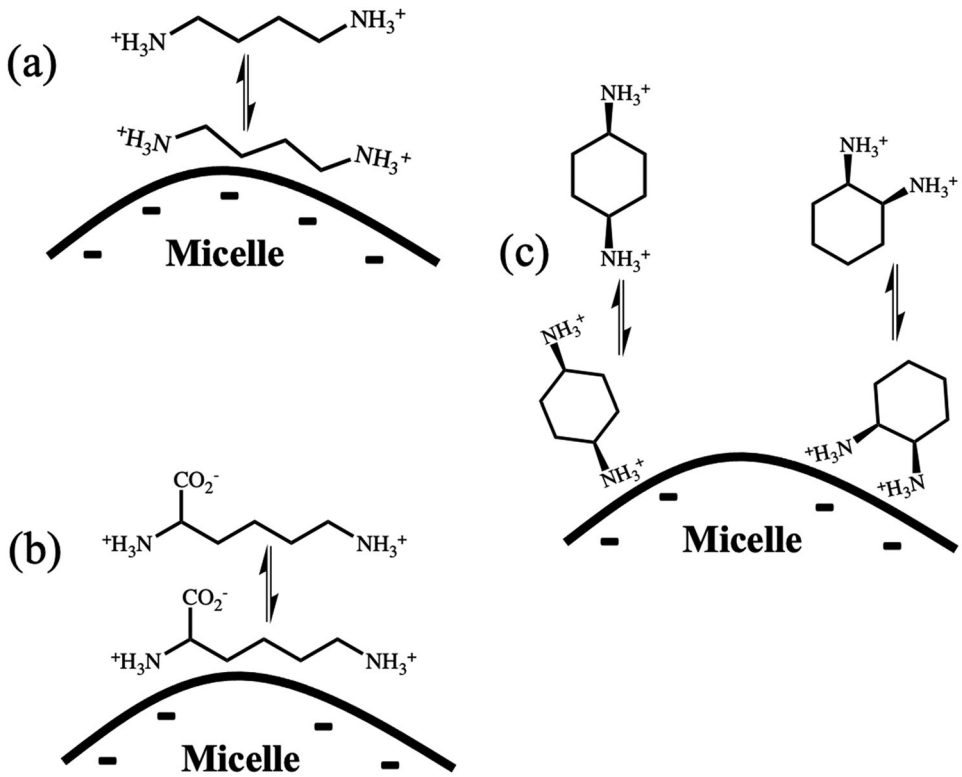

Figure 5. Models of (a) 1,4-diaminobutane, (b) L-Lysine, and (c) cyclohexanediamine isomers binding to the surface of und-LV micelles.

micelle instead of linking or bridging two or more micellar aggregates. If the latter occurred, the species diffusing in solution would be expected to have a radius much larger than 18–20 Å and diffusion coefficients smaller than those shown in Table 2. It is also interesting to note that at low pH $f_{b,counterion}$ is largest for 1,6-diaminohexane, smaller for 1,4-diaminobutane and smallest for L-Lysine. This result suggests that in 1,6-diaminohexane the spacings between amine functional groups and the flexibility of the longer methylene chain may allow this amine to interact more favorably with two surfactant monomers when compared to 1,4-diaminobutane. The fraction of bound counterion at low pH may also be smaller for L-Lysine because of the unfavorable repulsion that exists between the negative L-Lysine carboxylate functional group and the anionic micelle surface when the amino acid binds in a parallel fashion.

Further insight into the mode of cation binding to the micelles can be gained from an analysis of ROESY spectra for mixtures of und-LV and the diamines discussed above. In two-dimensional ROESY spectra, cross peaks connect NMR resonances for protons that are within approximately 5 Å of one another.[12,37] In intermolecular complexes, ROESY cross peaks are observed not only between protons within the same molecule, but also between protons of different molecules that are close to one another in space. The latter are referred to as intermolecular cross peaks.[12,37] The presence or absence of these intermolecular interactions can provide insight into the structures of intermolecular complexes like the micelle-counterion mixtures discussed above.[12,28,29] In this study, we applied the ROESY technique in a qualitative manner by using the presence, absence, and relative volumes of intermolecular ROESY cross peaks to support the model of parallel binding of the linear diamines and L-Lysine to the micelle surface. Quantitative ROESY analyses have also been reported in which changes in cross peak volume with mixing time are used to measure interatomic distances.[41–43] Finally, the complimentary information obtained by combining NMR diffusion and two-dimensional NMR experiments has been used by other researchers to gain insight into the structures of micellar aggregates and macromolecules.[44–46]

Figure 6a shows an expansion of the ROESY spectrum of a mixture containing und-LV and 1,4-diaminobutane at pH 7.5. Figures 2–4 in the Supplemental Information show full scale ROESY spectra for mixtures containing und-LV, the linear diamines, and L-Lysine. Table 2 shows that at this pH, $f_{b,counterion}$ is 0.48. In Figure 6a, the intermolecular cross peaks connecting the 1,4-diaminobutane resonances and the methyl protons of und-LV Leucine and Valine headgroup are identified by a red box. The presence of these intermolecular cross peaks between the und-LV methyl protons and both nonequivalent methylene 1,4-diaminobutane proton resonances suggests that these respective protons are within ~5 Ð of one another. Furthermore, the volumes of these intermolecular cross peaks are similar (12.49 and 14.39 for the cross peaks at 2.95 and 1.66 ppm in the f2 dimension, respectively) suggesting each pair of methylene resonances is at a comparable distance from the micelle surface. These intermolecular cross peaks, therefore, support the model of 1,4-diaminobutane binding parallel to the micelle surface because this mode of binding would place all the counterions methylene resonances at a comparable distance from the und-LV headgroup protons. If the counterion instead bound perpendicular to the surface, we would expect the

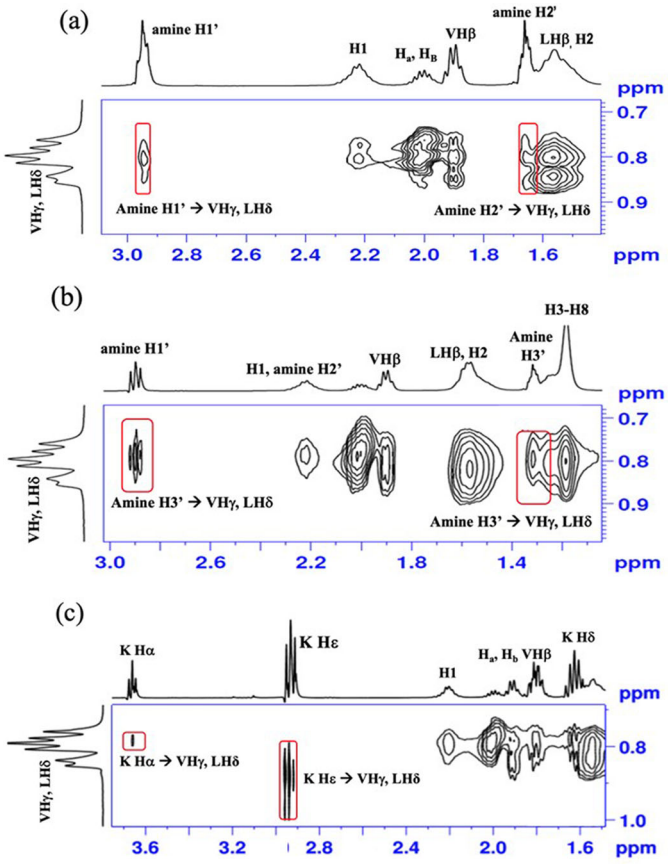

Figure 6. ROESY spectra for mixtures containing und-LV micelles and (a) 1,4-diaminobutane, (b) 1,6-diaminohexane, and (c) L-Lysine counterions.

counterion methylene resonances adjacent to the amine functional group to experience stronger ROESY interactions with the micelle headgroup protons than the methylene resonances at the center of the linear diamine. Since this result is not observed and since a modest change in R_h was observed when the counterion dissociated from the micelle surface, the ROESY and NMR diffusion techniques both support parallel counterion binding to und-LV micelles.

Figure 6b shows a ROESY spectrum for a mixture of und-LV and 1,6-diaminohexame at pH 7.5 ($f_{b,counterion}$ = 0.56). Again, the intermolecular cross peaks between the counterion and und-LV methyl protons are identified by a red box. The 1,6-diaminohexane counterion has three nonequivalent methylene resonances. Two of these resonances (H1′ and H3′) are well resolved and show intermolecular cross peaks with the und-LV headgroup resonances in Figure 6b. As with 1,4-diaminobutane, the volumes of these three cross peaks are similar at 39.1 and 41.7 for the cross peaks with chemical shifts of 2.90 and 1.32 ppm in the f2 dimension, respectively, suggesting that these methylene protons are at a comparable distance from the micelle surface. These ROESY cross peaks and the modest change in und-LV radius observed when 1,6-diaminohexane dissociates from the micelle suggest that 1,6-diaminohexane also binds parallel to the micelle surface with its two amine functional groups bridging two surfactant monomers.

Finally, the ROESY spectrum of a mixture containing und-LV and L-Lysine at pH 7.5 ($f_{b,counterion}$ = 0.33) is shown in Figure 6c. The cross peaks highlighted with a red box are between the und-headgroup methyl resonances and the Hα and Hε resonances of the L-Lysine counterion. These cross peaks are generally weaker than those observed for the linear diamines, likely in part because of the weaker overall binding of L-Lysine to the micelles. The presence of cross peaks for L-Lysine resonances adjacent to the molecule's primary and side chain amine functional groups again suggests parallel binding of L-Lysine to the micelle surface as was observed for the two linear diamines. Parallel binding of L-Lysine counterions has also been observed in mixtures containing this counterion and undecyl Leucinate and undecyl Phenylalaninate micelles.[28,29] In Figure 6c, ROESY spectrum, the volumes of these two cross peaks are different (8.92 and 18.78 for the resonances at 3.66 and 2.93 ppm in the f2 dimension, respectively), as might be expected since in L-Lysine there is a single Hα proton, but two equivalent Hε protons.

Cyclohexane diamines

NMR spectroscopy was also used to investigate the binding of the cis and trans isomers of both 1,4-diaminocyclohexane and 1,2-diaminocyclohexane to und-LV micelles. The structures of these amines are shown in Figure 1. pK_a values for 1,4-diaminocyclohexane are 9.4 and 10.8. For 1,2-diaminocyclohexane, pK_a values are 9.93 and 6.13 for the cis isomer and 9.94 and 6.47 for the trans isomer.[40,47] In the analyses of these mixtures, NMR spectra showed a counterion methyne resonance at approximately 3 ppm whose decay with increasing gradient strength was used to calculate the counterion diffusion coefficient. The other diaminocyclohexane proton resonances were overlapped either partially or completely by und-LV headgroup and hydrocarbon chain resonances. Therefore, unambiguous assignment of multiple intermolecular ROESY cross peaks could not be made and the development of the counterion-micelle binding models discussed below relied on results from the diffusion experiments.

The pK_a values for the 1,4-diaminocyclohexane isomers reported above suggest that the amine functional groups are both in protonated or ammonium form and that the counterion has a +2 charge below pH 9. The counterion deprotonates at higher pH, thus reducing its charge. In contrast, both 1,2-diaminocyclohexane isomers have pK_{a1} values in the 6–6.5 range and pK_{a2} values around 9.9. Therefore, from pH 7.5 − 9, the amine functional groups are expected to be in monoprotonated form giving the counterion an overall +1 charge. Again, deprotonation at higher pH reduces the counterion charge. Figure 4A and Table 3 show relatively strong counterion-micelle association below pH 9.5. For example, $f_{b,counterion}$ for trans and cis-1,4-diaminocyclohexane was 0.73 and 0.79, respectively, at pH 7.5. These values remain relatively constant in the 0.79–0.72 range until pH 9.5 when they begin to decrease and fall to near zero at pH 11.5. Therefore, as with the linear diamines and L-Lysine, the 1,4-diaminocyclohexane isomers are bound to the micelles in their cationic states but dissociate from the

micelle surface to be replaced by Na^+ cations at higher pH. D values used to calculate $f_{b,counterion}$ and R_h are given in Table 3 as well.

Furthermore, the micelle hydrodynamic radius changed by a generally larger amount when the 1,4-diaminocyclohexane isomers dissociated from the micelle surface compared to the corresponding change for the linear diamines and L-Lysine. For example, the micelle R_h changes from 20.4 Å at pH 7.5 to 10.8 Å at pH 11.5 in the mixture containing trans-1,4-diaminocyclohexane and from 20.4 Å at pH 7.5 to 9.9 Å at pH 11.5 for the und-LV-cis-1,4-diaminocylcohexane mixture. This observation suggests that the 1,4-cyclohexanediamine isomers bind perpendicular to the micelle surface with one amine functional group interacting with the anionic micelle surface and the rest of the molecule extending away from the surface and into solution. This model is shown in Figure 5c. Binding of the counterions in this fashion at low pH increases the micelle hydrodynamic radius because R_h represents the radius of the surfactant micelles and all bound counterions. When the counterion then deprotonated and dissociated from the micelle surface at high pH, a relatively large change in R_h resulted as observed in the above NMR radii measurements. The perpendicular packing model shown in Figure 5c for the 1,4-diaminocyclohexanes would also allow for a high coverage of the micelle surface with counterions because each counterion interacts with a single surfactant monomer. Figure 4A and 4B and Table 3 do in fact show that $f_{b,counterion}$ for both 1,4-diaminocyclohexane isomers is greater than 0.70 below pH 9. These are the largest $f_{b,counterion}$ values observed for the counterions in this study. Finally, if the counterions bound to the micelle surface as shown in Figure 5c, we would expect relatively little difference between the association of the cis- and trans-1,4-diaminocylcohexane isomers with the und-LV micelles. In other words, the relative orientation of the two amines would not likely affect micelle binding if only one amine functional group at a time interacted with the micelle surface. The $f_{b,counterion}$ values in Table 3 and Figure 4A and 4B do in fact show relatively little difference between the cis and trans isomers of 1,4-diaminocyclohexane.

Micelle hydrodynamic radii, $f_{b,counterion}$ values, and corresponding diffusion coefficients are also given in Table 4 for cis- and trans-1,2-diaminocyclohexane-und-LV mixtures. These values are plotted in Figure 4C and 4D, respectively. For trans-1,2-diaminocyclohexane, $f_{b,counterion}$ was in the range 0.44–0.40 between pH 7.5 and 9.5. The fraction of bound counterions decreased at higher pH to a value of 0.20 at pH 11.5. Similar behavior was seen with the cis-1,2-diaminocyclohexane counterion, where $f_{b,counterion}$ was in the range 0.56–0.44 from pH 7.5 to 9.0. This value again decreased at higher pH to a value of 0.12 at pH 11.5. Therefore, like the other counterions investigated, the 1,2-diaminocyclohexane isomers dissociated from the micelle surface when they deprotonated at higher pH.

Also, at low pH the $f_{b,counterion}$ values for the 1,2-diaminocylcohexane isomers are generally lower than corresponding values for 1,4-diaminocyclohexanes. For example, at pH 7.5 $f_{b,counterion}$ for trans-1,2-diaminocyclohexane is 0.44, whereas $f_{b,counterion}$ for trans-1,4-diaminocyclohexane is 0.72. A similar difference was seen for the cis isomers. This difference likely results in part from the pK_a values reported above, which suggest that below pH 10, the 1,4-diaminocylcohexane amine functional groups are both protonated and the molecule has a +2 charge. In contrast, the 1,2-diaminocyclohexane isomers are monoprotonated in this range and the charge of the counterion is +1. The lower charge of 1,2-diaminocyclohexane thus reduces its electrostatic attraction to the anionic micelles resulting in lower $f_{b,counterion}$ values. Furthermore, in their monoprotonated or +1 form, the 1,2-diaminocyclohexane isomers form intramolecular hydrogen bonds. These H-bonds have been investigated both theoretically and experimentally by Lopes Jesus, et al.[48] In the 1,2-diaminocyclohexane isomers, intramolecular hydrogen bond formation may compete with the formation of H-bonds between the counterion amine functional groups and und-LV headgroup atoms, thus reducing the $f_{b,counterion}$ values at lower pH. Intramolecular hydrogen bonding is expected to be less important in the 1,4-diaminocyclohexane isomers, especially at lower pH where both amine functional groups are in ammonium form. When the amine functional groups deprotonate at higher pH though, hydrogen bonding can occur in 1,4-diaminocyclohexane via the boat conformation of the cyclohexane ring.[48] Finally, as with Na^+, the linear diamines, and L-Lysine, $f_{b,LV}$ values for the diaminocyclohexanes remain near one over the pH range investigated.

Table 4 also shows that the change in the micelle hydrodynamic radius observed when the 1,2-diaminocyclohexane isomers dissociate from the micelle surface at high pH is comparable to that observed with the 1,4-diaminocyclohexane isomers. For example, in trans-1,2-diaminocylcohexane R_h decreases from 19.7 Å at pH 7.5 to 11.6 Å at pH 11.5. In cis-1,2-diaminocyclohexane, the corresponding change was from 18.4 Å at pH 7.5 to 10.5 Å at pH 11.5. This result suggests that, as shown in Figure 5c, the 1,2-diaminocyclohexane isomers bind perpendicular to the micelle surface with both amine functional groups interacting with the und-LV surfactant monomers. In addition, with the 1,2-diaminocyclohexane isomers, a small difference is observed between the $f_{b,counterion}$ values for the cis and trans isomers at low pH. For example, at pH 7.5 $f_{b,counterion}$ is 0.56 for the cis isomer and 0.44 for the trans isomer. Differences are also seen at pH 8.0 and 8.5 where in each case $f_{b,counterion}$ is larger for the cis isomer. These results suggest that in the cis isomer where the two amine functional groups are pointing in the same direction, the counterion can more easily interact simultaneously with the anionic headgroups of the und-LV surfactant monomers.

Conclusions

NMR spectroscopy was used to investigate the binding of Na^+, amine, and amino acid counterions to und-LV micelles. NMR methods were used because they probe both the structures and dynamics of micellar systems.[30–35] Our goal was to characterize the intermolecular interactions

present in solutions containing amino acid-based surfactants. These interactions affect the micelles' physical properties and their ability to bind differently to analyte enantiomers in chiral CE separations.[10,11,16,27,28] The NMR methods employed included diffusion studies to characterize micelle-counterion binding equilibria and 2D-NMR experiments to investigate the structures of counterion-micelle complexes. In solutions containing the und-LV micelles and Na^+ or $(C_2H_5)_4N^+$ counterions, the fraction of micelle-bound surfactant and counterion molecules along with the micelle hydrodynamic radii remained relatively constant as a function of pH. The linear diamines and L-Lysine were found to bind parallel to the und-LV micelle surface, with their amine functional groups interacting with multiple surfactant monomers. Both the linear diamines and L-Lysine dissociated from the micelle at higher pH. In contrast, NMR experiments suggested that the 1,2- and 1,4-diaminocyclohexane isomers bound perpendicular to the und-LV micelle surface with the amine functional groups interacting with a single surfactant monomer and the rest of the molecule extending into solution. Binding models for both the linear and cyclic diamines are shown in Figure 5. Furthermore, below pH 8, the mole fraction of micelle-bound 1,2-, and 1,4-diaminocyclohexane was higher than the linear diamines or L-Lysine. This difference was attributed partly to the perpendicular binding shown in Figure 5c which allowed for a high coverage of the micelle surface with counterions. Finally, the cis and trans isomers of 1,2-diaminocyclohexane had different $f_{b,counterion}$ values at low pH, whereas $f_{b,counterion}$ values for 1,4-diaminocyclohexane isomers were the same under these conditions.

Acknowledgments

We also acknowledge the generosity of the Ralph E. Klingenmeyer family.

Disclosure statement

The authors report that there are no competing interests to declare.

Funding

This work was supported by National Science Foundation-RUI Grants #1708959, #1709394, and #1709680 and by a Robert A. Welch Chemistry Departmental Grant to the Texas A&M University Corpus Christi Chemistry Program.

References

[1] Mikami, N.; Oota, R. Testing and Developing a Sugar-Derived Surfactant Blend for Delicate Skin. *SOFW J.* **2008**, *134*, 27–32. https://www.cosmeticsandtoiletries.com/testing/sensory/article/21835221/testing-and-developing-a-sugarderived-surfactant-blend-for-delicate-skin

[2] Bettenhausen, C. Switching to Sustainable Surfactants. *Chem. Eng. News* **2022**, *100*. 1–12. https://cen.acs.org/business/specialty-chemicals/Switching-sustainable-surfactants/100/i15

[3] Bordes, R.; Holmberg, K. Amino Acid Based Surfactants-Do They Deserve More Attention. *Adv. Colloid. Interface Sci.* **2015**, *222*, 79–91. DOI: 10.1126/sciadv.aao6494.

[4] Chandra, N.; Tyagi, V. K. Synthesis, Properties, and Applications of Amino Acids Based Surfactants: A Review. *J. Dispers. Sci. Technol.* **2013**, *34*, 800–808. DOI: 10.1080/01932691.2012.695967.

[5] Pinazo, A.; Pons, R.; Pérez, L.; Infante, M. R. Amino Acids as Raw Materials for Biocompatable Surfactants. *Ind. Eng. Chem. Res.* **2011**, *50*, 4805–4817. DOI: 10.1021/ie1014348.

[6] Greber, K. E. Synthesis and Surface Activity of Cationic Amino Acid Based Surfactants in Aqueous Solution. *J. Surfactants Deterg.* **2017**, *20*, 1189–1196. DOI: 10.1007/s11743-017-2002-4.

[7] Tadros, T. Surfactants. In *Encyclopedia of Colloid and Interface Science*, Tadros, T., Eds.; Springer: Berlin, Heidelberg, **2013**; pp 1242–1290. https://doi.org/10.1007/978-3-642-20665-8_40

[8] Pinheiro, L.; Faustino, C. *Amino Acid Based Surfactants for Biomedical Applications;* Najjar, R., Eds. InTechOpen: London, **2016**. https://www.intechopen.com/chapters/54704. DOI: 10.5772/67977.

[9] Pinazo, A.; Manresa, M. A.; Marques, A. M.; Bustelo, M.; Espuny, M. J.; Perez, L. Amino Acid Based Surfactants: New Antimicrobial Agents. *Adv. Colloid Interface Sci.* **2016**, *228*, 17–39. DOI: 10.1016/j.cis.2015.11.007.

[10] Billiot, E. J.; Macossay, J.; Thibodeaux, S.; Shamsi, S. A.; Warner, I. M. Chiral Separations Using Dipeptide Polymerized Surfactants: Effect of Amino Acid Order. *Anal. Chem.* **1998**, *70*, 1375–1381. DOI: 10.1021/Ac9709561.

[11] Shamsi, S. A.; Valle, B. C.; Billiot, F. H.; Warner, I. M. Polysodium N-undecanoyl-L-Leucylvalinate: A Versatile Chiral Selector for Micellar Electrokinetic Chromatography. *Anal. Chem.* **2003**, *75*, 379–387. DOI: 10.1021/Ac020386R.

[12] Morris, K. F.; Froberg, A. L.; Becker, B. A.; Almeida, V. K.; Tarus, J.; Larive, C. K. Using NMR to Develop Insights into Electrokinetic Chromatography. *Anal. Chem.* **2005**, *77*, 254A–263A. DOI: 10.1021/ac0534071.

[13] Morris, K. F.; Billiot, E. J.; Billiot, F. H.; Lipkowitz, K. B.; Southerland, W. M.; Gladis, A. A.; Fang, Y. A Molecular Dynamics Simulation Study of the Association of 1,1′-Binaphthyl-2, 2′-Diyl Hydrogenphosphate Enantiomers with a Chiral Molecular Micelle. *Chem. Phys.* **2014**, *439*, 36–43. DOI: 10.1016/j.chemphys.2014.05.004.

[14] Morris, K. F.; Billiot, E. J.; Billiot, F. H.; Hoffman, C. B.; Gladis, A. A.; Lipkowitz, K. B.; Southerland, W. H.; Fang, Y. Molecular Dynamics Simulation and NMR Investigation of the Association of the β-Blockers Atenolol and Propranolol with a Chiral Molecular Micelle. *Chem. Phys.* **2015**, *457*, 133–146. DOI: 10.1016/j.chemphys.2015.05.024.

[15] Rugutt, J. K.; Billiot, E., J.; Warner, I. M. NMR Study of the Interaction of Monomeric and Polymeric Chiral Surfactants with (*R*)- and (*S*)-1,1‘-Binaphthyl-2,2‘-Diyl Hydrogen Phosphate. *Langmuir* **2000**, *16*, 3022–3029. DOI: 10.1021/la990539e.

[16] McCarroll, M. E.; Billiot, F. H.; Warner, I. M. Fluorescence Anisotropy as a Measure of Chiral Recognition. *J. Am. Chem. Soc.* **2001**, *123*, 3173–3174. DOI: 10.1021/ja005604h.

[17] Kimaru, I. W.; Xu, Y.; McCarroll, M. E. Characterization of Chiral Interactions Using Fluorescence Anisotropy. *Anal. Chem.* **2006**, *78*, 8485–8490. DOI: 10.1021/ac061335n.

[18] Jansson, M.; Stilbs, P. A Comparative Study of Organic Counterion Binding to Micelles with the Fourier Transform NMR Self-Diffusion Technique. *J. Phys. Chem.* **1985**, *89*, 4868–4873. DOI: 10.1021/j100268a042.

[19] Koyama, M. Effect of Arginine as a Counterion on Surfactant Properties of Fatty Acid Salts. *J. Dispers. Sci. Technol.* **2005**, *26*, 785–789. DOI: 10.1081/DIS-200063107.

[20] Lima, F. S.; Cuccovia, I. M.; Horinek, D.; Amaral, L. Q.; Riske, K. A.; Schreier, S.; Salinas, R. K.; Bastos, E. L.; Pires, P. A. R.; Bozelli, J. C.; et al. Effect of Counterions on the Shape, Hydration, and Degree of Order at the Interface of Cationic Micelles: The Triflate Case. *Langmuir* **2013**, *29*, 4193–4203. DOI: 10.1021/la304658e.

[21] Fernandez-Alvarez, R.; Nová, L.; Uhlík, F.; Kereïche, S.; Uchman, M.; Košovan, P.; Matějíček, P. Interactions of Star-Like Polyelectrolyte Micelles with Hydrophobic Counterions. *J. Colloid Interface Sci.* **2019**, *546*, 371–380. DOI: 10.1016/j.jcis.2019.03.054.

[22] Talens-Alesson, F. The Role of Ionic Pair Association on Micellization and Counterion Binding in Ionic Micelles. *J. Phys. Chem. B* **2009**, *113*, 9779–9785. DOI: 10.1021/jp900928c.

[23] Rashidi-Alavijeh, M.; Javadian, S.; Gharibi, H.; Moradi, M.; Tehrani-Bagha, A. R.; Shahir, A. A. Intermolecular Interactions between a Dye and Cationic Surfactants: Effects of Alkyl Chain, Head Group, and Counterion. *Colloid Surf. A* **2011**, *380*, 119–127. DOI: 10.1016/j.colsurfa.2011.02.011.

[24] Gnezdilov, O. I.; Zuev, Y. F.; Zueva, O. S.; Potarikina, K. S.; Us'yarov, O. G. Self-Diffusion of Ionic Surfactants and Counterions in Premicellar and Micellar Solutions of Sodium, Lithium and Cesium Dodecyl Sulfates as Studied by NMR-Diffusometry. *Appl. Magn. Reson.* **2011**, *40*, 91–103. DOI: 10.1007/s00723-010-0185-1.

[25] Zuev, Y. F.; Gnezdilov, O. I.; Zueva, O. S.; Us'yarov, O. G. Effective Self-Diffusion Coefficients of Ions in Sodium Dodecyl Sulfate Micellar Solutions. *Colloid. J.* **2011**, *73*, 59–64. DOI: 10.1134/S1061933X11010224.

[26] Ramos, Z.; Rothbauer, G. A.; Turner, J.; Lewis, C.; Morris, K. F.; Billiot, E. J.; Billiot, F. H.; Fang, Y. Comparison of Chiral Recognition of Binaphthyl Derivatives with L-Undecyl-Leucine Surfactants in the Presence of Arginine and Sodium Counterions. *J. Chromatogr. Sci.* **2019**, *57*, 54–62. DOI: 10.1093/chromsci/bmy080.

[27] Garcia, M.; Risley, A.; Billiot, F. H.; Billiot, E. J.; Morris, K. F. Chiral Recognition of Binaphthyl Derivatives with L-Undecyl Leucine Surfactants in the Presence of Sodium and Lysine Counterions. *Am. J. Anal. Chem.* **2021**, *12*, 188–201. DOI: 10.4236/ajac.2021.125012.

[28] Lewis, C.; Hughes, B. H.; Vasquez, M.; Wall, A. M.; Northrup, V. L.; Witzleb, T. J.; Billiot, E. J.; Fang, Y.; Billiot, F. H.; Morris, K. F. Effect of pH on the Binding of Sodium, Lysine, and Arginine Counterions to L-Undecyl Leucinate Micelles. *J. Surfact Deterg.* **2016**, *19*, 1175–1188. DOI: 10.1007/s11743-016-1875-y.

[29] Rothbauer, G. A.; Rutter, E. A.; Reuter-Seng, C.; Vera, S.; Billiot, E. J.; Fang, Y.; Billiot, F. H.; Morris, K. F. Nuclear Magnetic Resonance Investigation of the Effect of pH on Micelle Formation by the Amino Acid-Based Surfactant Undecyl L-Phenylalaninate. *J. Surfactants Deterg.* **2018**, *21*, 139–153. DOI: 10.1002/jsde.12015.

[30] Stilbs, P. Fourier Transform Pulsed-Gradient Spin-Echo Studies of Molecular Diffusion. *Prog. Nucl. Mag. Reason. Spectrosc.* **1987**, *19*, 1–45. DOI: 10.1016/0079-6565(87)80007-9.

[31] Wong, T. C. Micellar Systems: Nuclear Magnetic Resonance Spectroscopy. In *Encyclopedia of Surface and Colloid Science*; Taylor & Francis: Boca Raton, FL, **2006**. DOI: 10.1081/E-ESCS-120023321.

[32] Evans, R.; Hernandez-Cid, A.; Dal Poggetto, G.; Vesty, A.; Haiber, S.; Morris, G. A.; Nilsson, M. Matrix-Assisted Diffusion-Ordered NMR Spectroscopy with an Invisible Matrix: A Vanishing Surfactant. *RSC Adv.* **2017**, *7*, 449–452. DOI: 10.1039/C6RA26144B.

[33] D'Errico, G.; Ortona, O.; Paduano, L.; Vitagliano, V. Transport Properties of Aqueous Solutions of Alkyltrimethylammonium Bromide Surfactants at 25 °C. *J. Colloid Interface Sci.* **2001**, *239*, 264–271. DOI: 10.1006/jcis.2001.7555.

[34] Chachaty, C. Applications of NMR Methods to the Physical Chemistry of Micellar Solutions. *Prog. Nucl. Magn. Reason. Spectrosc.* **1987**, *19*, 183–222. DOI: 10.1016/0079-6565(87)80002-X.

[35] Stilbs, P. *Diffusion and Electrophoretic NMR*; Walter de Gruyter: Boston, MA, **2019**. DOI: 10.1515/9783110551532.

[36] Wu, D.; Chen, A.; Johnson, C. S. Jr., An Improved Diffusion-Ordered Spectroscopy Experiment Incorporating Bipolar-Gradient Pulses. *J. Magn. Reson* **1995**, *115*, 260–264. DOI: 10.1006/jmra.1995.1176.

[37] Bax, A.; Davis, D. G. Practical Aspects of Two-Dimensional Transverse NOE Spectroscopy. *J. Magn. Reason* **1985**, *63*, 207–213. DOI: 10.1016/0022-2364(85)90171-4.

[38] Piotto, M.; Saudek, V.; Sklenár, V. Gradient-Tailored Excitation for Single-Quantum NMR Spectroscopy of Aqueous Solutions. *J. Biomol. NMR* **1992**, *2*, 661–665. DOI: 10.1007/BF02192855.

[39] Wilkins, D. K.; Grimshaw, S. B.; Receveur, V.; Dobson, C. M.; Jones, J. A.; Smith, L. J. Hydrodynamic Radii of Native and Denatured Proteins Measured by Pulse Field Gradient NMR Techniques. *Biochemistry* **1999**, *38*, 16424–16431. DOI: 10.1021/bi991765q.

[40] *CRC Handbook of Chemistry and Physics*; 103rd ed.; Rumble, J., Ed. CRC Press, Boca Raton, FL, **2021**. DOI: 10.1021/ja041017a.

[41] Ammalahti, E.; Bardet, M.; Molko, D.; Cadet, J. Evaluation of Distances from ROESY Experiments with the Intensity-Ratio Method. *J. Magn. Reason. A* **1996**, *122*, 230–232. DOI: 10.1006/jmra.1996.0199.

[42] Hilton, B. D.; Chmurny, G. N.; Muschik, G. M. Taxol: Quantitative Internuclear Proton-Proton Distances in $CDCl_3$ Solution from nOe Data: 2D NMR Roesy Buildup Rates at 500 MHz. *J. Nat. Prod.* **1992**, *55*, 1157–1161. DOI: 10.1021/np50086a023.

[43] Ganjiwale, A.; Cowsik, S. M. Membrane-Induced Structure of Novel Human Tachykinin Hemokinin-1 (hHK1). *Biopolymers* **2015**, *103*, 702–710. DOI: 10.1002/bip.22734.

[44] Jeannerat, D.; Furrer, J. NMR Experiments for the Analysis of Mixtures: Beyond 1D ^{1}H Spectra. *Comb. Chem. High Throughput Screen* **2012**, *15*, 15–35. DOI: 10.2174/138620712798280853.

[45] Pessine, F. B. T.; Calderini, A.; Alexandrino, G. L. *Magnetic Resonance Spectroscopy*; Kim, D., Ed.; IntechOpen: London, **2011**. www.intechopen.com/chapters/30457. DOI: 10.5772/1228.

[46] Fernandes, S. A.; Cabeca, L. F.; Marsaioli, A. J.; Paula, E. Investigation of Tetracaine Complexation with Beta-Cyclodextrins and *p*-Sulphonic Acid Calix[6]Arenes by nOe and PGSE NMR. *J. Incl. Phenom. Macrocycl. Chem.* **2007**, *57*, 395–401. DOI: 10.1007/s10847-006-9224-9.

[47] Armarego, W. L. F.; Chai, C. L. L. *Purification of Lab Chemicals;* 6th ed.; Elsevier, Burlington, VT, **2009**. www.intechopen.com/chapters/30457. DOI: 10.1016/C2009-0-64000-9.

[48] Lopes Jesus, J.; Helena, M.; Teixeira, S. F.; Redinha, J. S. Structure of Charged Cyclohexyldiamines in Aqueous Solution: A Theoretical and Experimental Study. *J. Phys. Chem. B* **2012**, *116*, 5019–5027. DOI: 10.1021/jp3011712.